Journal of Alloys and Compounds 370 (2004) 149–158

Journal of ALLOYS AND COMPOUNDS

www.elsevier.com/locate/jallcom

Thermodynamic assessment of the Ti–B system

Xiaoyan Ma, Changrong Li*, Zhenmin Du, Weijing Zhang

School of Materials Science and Engineering, University of Science and Technology Beijing, Beijing 100083, PR China

Received 8 July 2003; accepted 3 September 2003

Abstract

A consistent thermodynamic data set for the Ti–B system is obtained by means of CALPHAD technology. The sublattice model is used to describe the solid solution phases: $(Ti\%)_1(B, Va\%)_{0.5}$ and $(Ti\%)_1(B, Va\%)_3$ for the terminal solution (αTi) and (βTi), and $Ti_1(B\%, Ti)_1$ and $(B, Ti\%)_1(B\%, Ti)_2$ for the compound solution TiB and TiB_2, respectively. The intermetallic compound Ti_3B_4 is treated as a stoichiometric compound. The liquid solution phase is assumed to be a substitutional solution with Redlich–Kister formula for the expression of its excess Gibbs energy. The complete *T–x* phase diagram for the Ti–B binary system is given. The calculation results agree well with experiments.

Keywords: Ti–B binary; Phase diagram; Assessment

1. Introduction

Both TiB and TiB_2 exhibit extreme hardness, high electrical conductivity, good thermal shock resistance, high melting point, chemical inertness, and durability. They are widely used in such areas as crucibles, electrode materials, and protective coatings [1–4].

Ti–B system has been assessed by Murray et al. [5] and Bätzner [6], but both of them treated the compound solution phases TiB and TiB_2 as the stoichiometric compounds. A homogeneity range for TiB around 49–50 at.% B was observed [7–10]. The composition variation for TiB_2 was also found around 65.5–67 at.% B from Fenish [8], 65.2–66.3 at.% B from Rudy and Windisch [9] and 65.5–67.6 at.% B from Thebault et al. [10]. The small variation of lattice parameters also confirms the narrow homogeneity range of TiB_2 [11]. So, it is necessary to reassess the Ti–B system, especially considering the homogeneity ranges of the compound solutions TiB and TiB_2. The present assessment is on the basis of [5,6].

2. Experimental and estimated data from the literature

Ti–B binary system mainly includes the following phases:

- *the liquid solution phase*;
- *terminal solid solutions*: (αTi) phase, the solution of B in hcp Ti; (βTi) phase, the solution of B in bcc Ti; and (βB) phase, the solution of Ti in beta-rhombohedral-B;
- *compound solutions*: TiB and TiB_2;
- *stoichiometric compound*: Ti_3B_4.

The experimental phase diagram data are summarized in Table 1. The related crystal structures and lattice parameters are listed in Table 2. Murray et al. [5] gave a review for the phase diagram and the selected thermodynamic data. Additional aspects will be discussed in the following sections.

2.1. Phase diagram

2.1.1. Ti-rich alloys

There is only a small solid solubility of boron in (αTi). Utilizing metallography, Ogden and Jaffee [12] found that the solubility of B in (αTi) near the pure metal transformation temperature of 1155 K is less than 1.7 at.% B. With the same method, Palty et al. [13] found the temperature of the three-phase reaction of (βTi), (αTi), and TiB is 1159 ± 4 K and the solubility of B in (αTi) is less than 0.2 at.% B. The type of this three-phase reaction is peritectic [9,13].

The solubility of B in (βTi) is also very small. The value of <1 at.% B was given by Rudy and Windisch [9] and about 0.1 at.% B by Palty et al. [13]. The solidification occurs by the eutectic reaction, liquid ↔ (βTi) + TiB. There is

* Corresponding author.
E-mail address: fuming@public.fhnet.cn.net (C. Li).

0925-8388/$ – see front matter © 2003 Elsevier B.V. All rights reserved.
doi:10.1016/j.jallcom.2003.09.017

Table 1
Experimental phase diagram data of the Ti–B system[a]

Type of data	Method	Value	Reference	
Solubility of B in (αTi)	Metallography	1155 K <1.7 at.% B	[12]	+
	Metallography	1159 ± 4 K <0.2 at.% B	[13]	−
Solubility of B in (βTi)	Metallography	1813 ± 10 K <1 at.% B	[9]	+
	Metallography	1943 ± 25 K ~0.1 at.% B	[13]	−
Melting point of TiB	Metallography	2463 ± 25 K	[9]	+
	Metallography	2333 K	[13]	−
		2173 ± 50 K	[15]	−
Homogeneity of TiB	Metallography	49–50 at.% B	[7–9]	+
		45.8–49.3 at.% B	[10]	+
Existence of Ti_3B_4	Metallography	57.14%	[8]	+
	X-ray diffraction		[17]	+
	Electron microscopy		[18]	+
	Arc-melting and annealing studies		[19]	+
Melting point of TiB_2	Metallography	>3153 K	[8]	−
	Metallography	3498 ± 25 K	[9]	+
		3123 ± 50 K	[20]	−
		3173 ± 80 K	[21]	−
		3063 K	[22]	−
		3193 ± 30 K	[15,23]	−
		3498 K	[24]	+
Homogeneity of TiB_2	Metallography	65.5–67at.% B	[8]	+
	Metallography	65.2–66.3at.% B	[9]	+
	X-ray diffraction	65.5–67.6 at.% B	[10]	+
Eutectic reaction, liquid ↔ TiB_2 + (βB)	Metallography	2353 ± 20 K >98 at.% B	[9]	+

[a] The last column indicates that the data were used (+) or not used (−) in the present assessment.

a disagreement about the eutectic composition between Fenish [8] (<1 at.% B) and Rudy and Windisch [9] (7 ± 1 at.% B). According to the prediction equation made from the application of the Van't Hoff relationship for the dilute region and suggested by Okamoto and Massalski [14], the initial slope of liquidus is calculated and shown in Fig. 1, where the solidus is treated as vertical. The data of Rudy and Windisch [9]and Fenish [8] are also plotted in the same figure. Since the data of Fenish [8] is so different from the present prediction, it was not used in the assessment. The eutectic temperature was reported as (1813 ± 10) [9], (1803 ± 10) [8], and (1943 ± 25) K [13]. The latter value does not used in the assessment because of the probability of specimen contamination [5].

Table 2
Crystal structures and lattice parameters of the Ti–B system

Phase	Pearson symbol	Space group	Struktur–Bericht designation	Prototype	Lattice parameters (nm)			Reference
					a	*b*	*c*	
(αTi)	*hP*2	$P6_3/mmc$	*A*3	Mg	–	–	–	[28]
(βTi)	*cI*2	*Im*3*m*	*A*2	W	–	–	–	[28]
TiB	*oP*8	*Pnma*	*B*27	FeB	0.612	0.306	0.456	[7]
					0.6105	0.3048	0.4542	[16]
TiB_2	*hP*3	*P*6/*mmm*	*C*32	AlB_2	0.3028–0.3040	–	0.3228–0.3234	[11]
					0.3028	–	0.3230	[29]
					0.3030	–	0.3228	[30]
Ti_3B_4	*oI*14	*Immm*	$D7_b$	Ta_3B_4	0.3259	1.373	0.3042	[17]
					0.3260	1.372	0.3041	[19]
(βB)	*hR*108	$R\bar{3}m$	–	(βB)	1.09251	–	2.3814	[31]

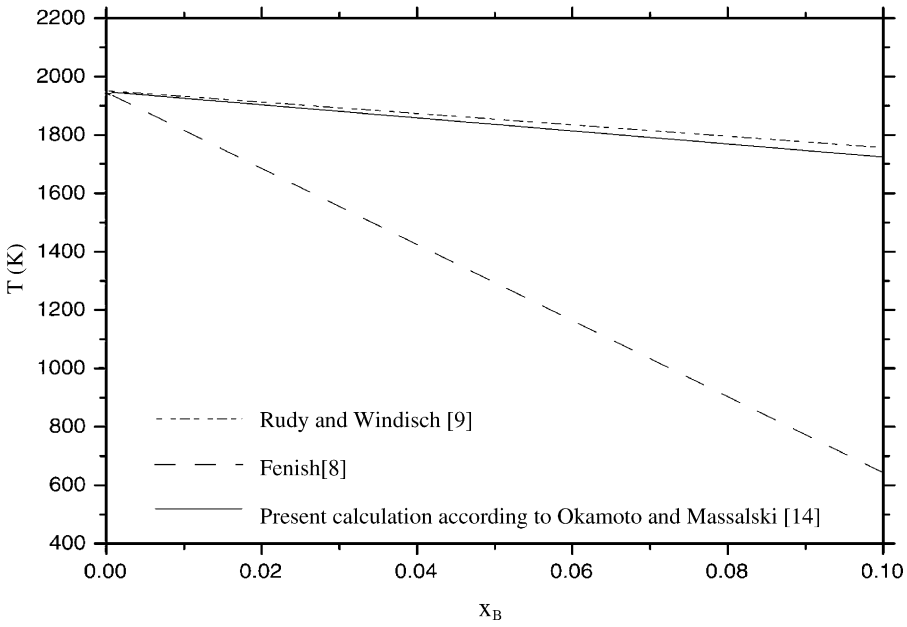

Fig. 1. Initial slope of liquidus when solidus is vertical.

2.1.2. TiB

By melting point and metallographic examinations [7–9,13,15], and by structural studies [9,16], the existence of the TiB was confirmed and it forms by a peritectic reaction. But there is a disagreement between Fenish [8] and Rudy and Windisch [9] on whether the reaction is liquid + Ti_3B_4 ↔ TiB at 2273 K [8] or liquid + TiB_2 ↔ TiB at 2463 ± 25 K [9].

According to [7–9], there is a narrow homogeneity range around 49–50 at.% B. Thebault et al. [10] found this homogeneity range is from 45.8 to 49.3 at.% B by studying B fiber–Ti composite materials.

2.1.3. Ti_3B_4

Using different methods, the existence of Ti_3B_4 was confirmed by several groups of authors, metallographic study by Fenish [8], X-ray diffraction by Fenish [17], electron microscopy by Neronov et al. [18], and arc-melting and annealing studies by Spear et al. [19]. The crystal structure of Ti_3B_4 was reported as Ta_3B_4 [17,19]. Fenish [8] also found two different forms of Ti_3B_4, low-temperature form and high-temperature form and the transformation occurs at 2283 K. But this transformation is irreversible. This means the specimen may be contaminated. So in the assessed phase diagram, only one form of Ti_3B_4 is used with the same structure for the high- and low-temperature of Ti_3B_4.

Fenish [8] reported that Ti_3B_4 forms by the peritectic reaction, liquid + TiB_2 ↔ Ti_3B_4, at 2293K while another peritectic reaction, liquid + Ti_3B_4 ↔ TiB, is at 2273 K. There is only 20 K of separation between these two peritectic reactions. Although Rudy and Windisch [9] did not find the existence of Ti_3B_4, but he found TiB had different etching properties in two different processes. One was by the peritectic reaction with TiB_2 and another was by primary solidification. According to Fenish [8], the reaction temperatures of the two reactions mentioned before are very close, 2293 and 2273 K, and the composition of Ti_3B_4 is also close to that of TiB. So, Rudy and Windisch [9] may be find two different phases. The further experiment on these two reactions is needed. In the assessed phase diagram, both reactions are considered.

2.1.4. TiB_2

There is a disagreement about the congruent melting temperature of TiB_2 [8,9,15,20–24]. These data are listed in Table 1. According to Murray et al. [5], the highest reported congruent temperature, 3498 K, is chosen in the assessed phase diagram.

By metallographic studies, a homogeneity range of TiB_2 was also observed by different measurements [8–10] as mentioned in the introductory section. The detailed data items are listed in Table 1. The small varieties of lattice parameters [11] in Table 2 correspond to the narrow homogeneity range. In the assessed phase diagram, the range is taken from 65 to 67.6 at.% B.

2.1.5. B-rich alloys

Rudy and Windisch [9] reported the eutectic reaction, liquid ↔ TiB_2 + (βB) at 2353±20 K, with the eutectic composition more than 98 at.% B. Since the solubility of Ti in (βB) is very low, the terminal solution phase (βB) was treated as pure element B in the assessment.

2.1.6. Metastable phases

Ti_2B_5 [15,22,25,26], TiB_x (TiB_{10} or TiB_{12}) [27] and Ti_2B [25] were also reported but none of them were detected by

the same investigation at one time. Furthermore, later researchers [8,9] did not observe those phases. In this assessment, they are not included.

2.2. Crystal structure and lattice parameter

Murray et al. [5] have summarized the crystal structures and lattice parameters of Ti–B system as listed in the Table 2.

The structure of TiB was treated as the zincblende [32] and the NaCl structure [33] but later researchers confirmed the orthorhombic FeB structure [7–9,16].

The structure of TiB_2 is of the AlB_2 type, which was verified by lots of studies [8,9,11,13,29,30,32–34].

The structure of Ti_3B_4 is of the Ta_3B_4 type [8,17,19].

2.3. Thermodynamic data

The experimental thermodynamic data for TiB and TiB_2 from literatures are summarized in Table 3.

Numerous researchers have studied the heat contents of stoichiometric TiB_2 at different range of temperature [36–41]. Chase [35] assessed these data and estimated the heat capacities for stoichiometric TiB (from 298.15 to 4000 K).

Schissel and Trulson [42] calculated the entropy of stoichiometric TiB at 298 K. Chase [35] presented the evaluated data of the entropy of stoichiometric TiB_2, which was calculated later by Yurick and Spear [1] using the second and third thermodynamic laws.

The heat formation of stoichiometric TiB_2, $\Delta^\circ H_f^{TiB_2}$ (298 K), was determined using X-ray diffraction [2,26,43,44] and mass spectrometer [42,45] experimentally and was calculated using the second and third thermodynamic laws [1] theoretically. From the experimental data of TiB_2, Schissel and Trulson [42] estimated the heat of formation of stoichiometric TiB, $\Delta^\circ H_f^{TiB}$(298 K). The data from Schissel and Trulson [42] are unreliable since the obvious contamination of specimen and they were not considered in the assessment.

No thermodynamic data can be obtained for other phases.

3. Thermodynamic models

3.1. Elements

The Gibbs energy function ${}^\circ G_i^\varphi(T) = G_i^\varphi(T) - H^{SER}(298.15\,K)$ for the pure element i in the φ phase is described by the equation:

$$
\begin{aligned}
{}^\circ G_i^\varphi(T) &= G_i^\varphi(T) - H^{SER}(298.15\,K) \\
&= a + bT + cT\ln T + dT^2 + eT^{-1} \\
&\quad + fT^3 + gT^7 + hT^{-9}
\end{aligned}
\tag{1}
$$

where H^{SER} (298.15 K) is the molar enthalpy of the stable element reference at 298.15 K and 101325 Pa, T the absolute temperature, and a, b, c, d, e, f, g, h are coefficients. In this work, the data for elements B and Ti were taken from Dinsdale [46].

Table 3
Experimental thermodynamic data of the Ti–B system[a]

Type of data	Method	Value (K)	Reference	
C_p for TiB ($J\,mol^{-1}\,K^{-1}$)			[35]	+
C_p for TiB_2 ($J\,mol^{-1}\,K^{-1}$)			[35]	+
	Drop calorimeter		[36]	+
			[37]	−
	Copper-block drop calorimeter		[38]	−
			[39]	−
			[40]	−
			[41]	−
$S_{298\,K}$ for TiB ($J\,mol^{-1}\,K^{-1}$)		34.7 ± 6.3	[42]	+
$S_{298\,K}$ for TiB_2 ($J\,mol^{-1}\,K^{-1}$)	Second law analysis	23.1 ± 8.4	[1]	−
	Third law analysis	28.602 ± 0.42	[1]	+
		28.48 ± 0.4	[35]	+
$H_{298\,K}$ for TiB ($J\,mol^{-1}$)		−160247	[42]	+
$H_{298\,K}$ for TiB_2 ($J\,mol^{-1}$)	Second law analysis	−314754 ± 17556	[1]	+
	Third law analysis	−305340 ± 6720	[1]	+
	X-ray diffraction	−323800	[2]	+
	X-ray diffraction	−298200	[26]	+
	Mass spectrometer	−217320	[42]	−
	X-ray diffraction	−292600	[43]	+
	X-ray diffraction	−319788	[44]	+
	Mass spectrometer	−300960	[45]	+

[a] The last column indicates that the data were used (+) or not used (−) in the present assessment.

3.2. Liquid phase

The substitutional solution model was chosen for the liquid phase:

$$G_{\mathrm{m}}^{\mathrm{L}}(T) - H^{\mathrm{SER}}(298.15\,\mathrm{K}) = {}^{\mathrm{ref}}G^{\mathrm{L}} + {}^{\mathrm{id}}G^{\mathrm{L}} + {}^{\mathrm{ex}}G^{\mathrm{L}} \quad (2)$$

where

$${}^{\mathrm{ref}}G^{\mathrm{L}} = x_{\mathrm{B}}{}^{\circ}G_{\mathrm{B}}^{\mathrm{L}}(T) + x_{\mathrm{Ti}}{}^{\circ}G_{\mathrm{Ti}}^{\mathrm{L}}(T) \quad (3)$$

$${}^{\mathrm{id}}G^{\mathrm{L}} = RT[x_{\mathrm{B}}\ln(x_{\mathrm{B}}) + x_{\mathrm{Ti}}\ln(x_{\mathrm{Ti}})] \quad (4)$$

$$\begin{aligned}{}^{\mathrm{ex}}G^{\mathrm{L}} = x_{\mathrm{B}}x_{\mathrm{Ti}}[&{}^{0}L_{\mathrm{B,Ti}}^{\mathrm{L}} + {}^{1}L_{\mathrm{B,Ti}}^{\mathrm{L}}(x_{\mathrm{B}} - x_{\mathrm{Ti}}) \\ &+ {}^{2}L_{\mathrm{B,Ti}}^{\mathrm{L}}(x_{\mathrm{B}} - x_{\mathrm{Ti}})^2 + {}^{3}L_{\mathrm{B,Ti}}^{\mathrm{L}}(x_{\mathrm{B}} - x_{\mathrm{Ti}})^3 + \cdots]\end{aligned} \quad (5)$$

${}^{\mathrm{ref}}G^{\mathrm{L}}$ is referred to the mechanical mixture of the pure elements in the liquid phase at temperature T, ${}^{\mathrm{id}}G^{\mathrm{L}}$ the ideal entropy of mixing, and ${}^{\mathrm{ex}}G^{\mathrm{L}}$ the excess Gibbs energy term.

x_{B} and x_{Ti} are the mole fraction of B and Ti in the liquid phase, respectively. The interaction parameters ${}^{i}L_{\mathrm{B,Ti}}^{\mathrm{L}}(i = 0, 1, 2, 3, \ldots)$ are again the function of temperature, $a_i + b_i T$. Eq. (5) is often referred to as the Redlich–Kister equation.

3.3. (βTi) and (αTi) solid solution phases

In the analogous system, Ti–N binary [47], (βTi) phase and (αTi) phase were described with the two-sublattice model developed by Hillert and Staffansson [48] and can be express by the general formula $(\mathrm{Ti\%})_1(\mathrm{N, Va\%})_a$. Va denotes vacancy, % the major component in the related sublattice. The subscript a is the number of interstitial sites per Ti atom, which is equal to 3 for (βTi) and 0.5 for (αTi). The same descriptions are adopted in this assessment $(\mathrm{Ti\%})_1(\mathrm{B, Va\%})_a$ ($a = 3$ and 0.5).

If φ denotes one of the phases, (βTi) or (αTi), the Gibbs energy per mole of formula unit is given by

$$\begin{aligned}&G_{\mathrm{m}}^{\varphi}(T) - H^{\mathrm{SER}}(298.15\,\mathrm{K}) \\ &= y_{\mathrm{Va}}{}^{\circ}G_{\mathrm{Ti}}^{\varphi}(T) + y_{\mathrm{B}}{}^{\circ}G_{\mathrm{Ti:B}_a}^{\varphi}(T) \\ &\quad + aRT(y_{\mathrm{Va}}\ln y_{\mathrm{Va}} + y_{\mathrm{B}}\ln y_{\mathrm{B}}) \\ &\quad + y_{\mathrm{B}}y_{\mathrm{Va}}[{}^{0}L_{\mathrm{Ti:B,Va}}^{\varphi} + (y_{\mathrm{B}} - y_{\mathrm{Va}}){}^{1}L_{\mathrm{Ti:B,Va}}^{\varphi} + \cdots]\end{aligned} \quad (6)$$

where y_{Va} and y_{B} denote site fractions of vacancy and boron in the second sublattice. ${}^{\circ}G_{\mathrm{Ti}}^{\varphi}(T)$ represents the Gibbs energy of pure titanium in φ (φ = (βTi) or (αTi)) modification, ${}^{\circ}G_{\mathrm{Ti:B}_a}^{\varphi}(T)$ the Gibbs energy of the hypothetical boride also in φ modification. The ${}^{i}L_{\mathrm{Ti:B,Va}}^{\varphi}(i = 0, 1, \ldots)$ parameters represent the interaction parameters between the element B and Va in the second sublattice with the first sublattice occupied by Ti.

3.4. Compound solution phase TiB

The sublattice model $(\mathrm{Ti\%})_1(\mathrm{B\%, Ti})_1$ is used for compound solution phase TiB. Its molar Gibbs energy is given by the following expression:

$$\begin{aligned}&G_{\mathrm{m}}^{\mathrm{TiB}}(T) - H^{\mathrm{SER}}(298.15\,\mathrm{K}) \\ &= y_{\mathrm{B}}{}^{\circ}G_{\mathrm{Ti:B}}^{\mathrm{TiB}}(T) + y_{\mathrm{Ti}}{}^{\circ}G_{\mathrm{Ti:Ti}}^{\mathrm{TiB}}(T) \\ &\quad + RT(y_{\mathrm{B}}\ln y_{\mathrm{B}} + y_{\mathrm{Ti}}\ln y_{\mathrm{Ti}}) + y_{\mathrm{B}}y_{\mathrm{Ti}}({}^{0}L_{\mathrm{Ti:B,Ti}}^{\mathrm{TiB}} + \cdots)\end{aligned} \quad (7)$$

where y_{B} and y_{Ti} denote site fractions of boron and titanium in the first sublattice, ${}^{\circ}G_{\mathrm{Ti:B}}^{\mathrm{TiB}}(T)$ the Gibbs energy of the stoichiometric compound TiB and ${}^{\circ}G_{\mathrm{Ti:Ti}}^{\mathrm{TiB}}(T)$ the Gibbs energy of the hypothetical compound TiTi with the same structure as TiB. Both of them take the same expression as for pure element, Eq. (1). The value of $c, d, e, f, \ldots$ in the ${}^{\circ}G_{\mathrm{Ti:B}}^{\mathrm{TiB}}(T)$ can be derived from C_p(TiB), and a and b are mainly determined by the standard heat of formation $\Delta^{\circ}H_{\mathrm{f}}^{\mathrm{TiB}}(298\,\mathrm{K})$ and entropy at 298 K $S_{298\,\mathrm{K}}$, respectively.

3.5. Compound solution phase TiB_2

The sublattice $(\mathrm{B, Ti\%})_1(\mathrm{B\%, Ti})_2$ is used for compound solution TiB_2 phase. Its molar Gibbs energy is given by the following expression:

$$\begin{aligned}&G_{\mathrm{m}}^{\mathrm{TiB_2}}(T) - H^{\mathrm{SER}}(298.15\,\mathrm{K}) \\ &= y'_{\mathrm{B}}y''_{\mathrm{B}}{}^{\circ}G_{\mathrm{B:B_2}}^{\mathrm{TiB_2}}(T) + y'_{\mathrm{B}}y''_{\mathrm{Ti}}{}^{\circ}G_{\mathrm{B:Ti_2}}^{\mathrm{TiB_2}}(T) \\ &\quad + y'_{\mathrm{Ti}}y''_{\mathrm{B}}{}^{\circ}G_{\mathrm{Ti:B_2}}^{\mathrm{TiB_2}}(T) + y'_{\mathrm{Ti}}y''_{\mathrm{Ti}}{}^{\circ}G_{\mathrm{Ti:Ti_2}}^{\mathrm{TiB_2}}(T) \\ &\quad + RT[(y'_{\mathrm{B}}\ln y'_{\mathrm{B}} + y'_{\mathrm{Ti}}\ln y'_{\mathrm{Ti}}) \\ &\quad + 2(y''_{\mathrm{Ti}}\ln y''_{\mathrm{Ti}} + y''_{\mathrm{B}}\ln y''_{\mathrm{B}})] + {}^{E}G_{\mathrm{m}}^{\mathrm{TiB_2}}\end{aligned} \quad (8)$$

$$\begin{aligned}{}^{E}G_{\mathrm{m}}^{\mathrm{TiB_2}} = &y'_{\mathrm{B}}y'_{\mathrm{Ti}}(y''_{\mathrm{B}}{}^{0}L_{\mathrm{B,Ti:B}}^{\mathrm{TiB_2}} + y''_{\mathrm{Ti}}{}^{0}L_{\mathrm{B,Ti:Ti}}^{\mathrm{TiB_2}}) \\ &+ y''_{\mathrm{B}}y''_{\mathrm{Ti}}(y'_{\mathrm{B}}{}^{0}L_{\mathrm{B:B,Ti}}^{\mathrm{TiB_2}} + y'_{\mathrm{Ti}}{}^{0}L_{\mathrm{Ti:B,Ti}}^{\mathrm{TiB_2}})\end{aligned} \quad (9)$$

where y'_{B} and y'_{Ti} denote site fractions of boron and titanium in the first sublattice, y''_{B} and y''_{Ti} site fractions of boron and titanium in the second sublattice. ${}^{\circ}G_{\mathrm{B:B_2}}^{\mathrm{TiB_2}}(T)$, ${}^{\circ}G_{\mathrm{B:Ti_2}}^{\mathrm{TiB_2}}(T)$, and ${}^{\circ}G_{\mathrm{Ti:Ti_2}}^{\mathrm{TIB_2}}(T)$ represent the Gibbs energy of the hypothetical compound BB_2, BTi_2, and $TiTi_2$, respectively. ${}^{\circ}G_{\mathrm{Ti:B_2}}^{\mathrm{TiB_2}}(T)$ is the Gibbs energy of the stoichiometric compound TiB_2.

3.6. Stoichiometric Ti_3B_4

There is no experimental data for standard heat of formation $\Delta^{\circ}H_{\mathrm{f}}^{\mathrm{Ti_3B_4}}(298\,\mathrm{K})$, entropy at 298 K $S_{298\,\mathrm{K}}$, and heat capacity $C_p(T)$ for stoichiometric Ti_3B_4. The following model for the Gibbs energy of Ti_3B_4 was used in the assessment:

$$\begin{aligned}&G_{\mathrm{m}}^{\mathrm{Ti_3B_4}}(T) - H^{\mathrm{SER}}(298.15\,\mathrm{K}) \\ &= a^{\mathrm{Ti_3B_4}} + b^{\mathrm{Ti_3B_4}}T + c^{\mathrm{Ti_3B_4}}T\ln T \\ &\quad + 4{}^{\circ}G_{\mathrm{B}}^{\beta}(T) + 3{}^{\circ}G_{\mathrm{Ti}}^{\mathrm{hcp}}(T)\end{aligned} \quad (10)$$

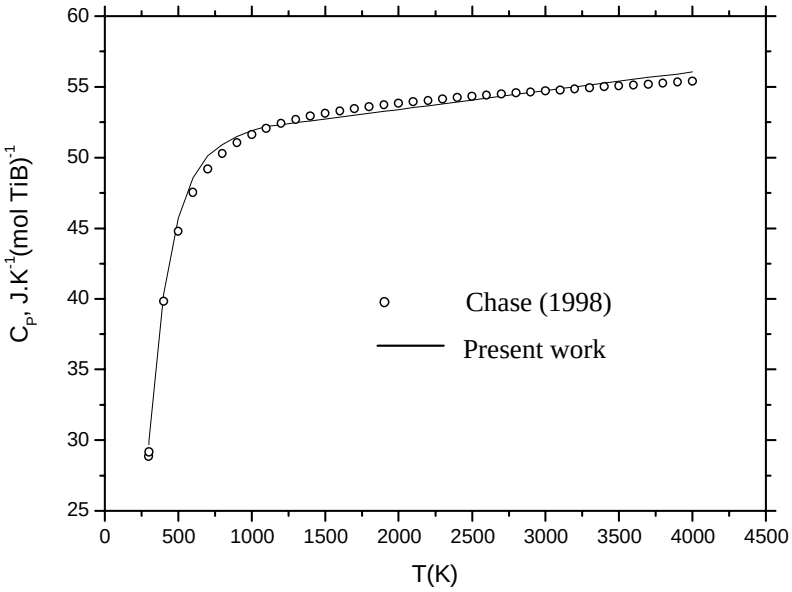

Fig. 2. Heat capacity of stoichiometric TiB compared with literature data [35].

3.7. βB

Since the solubility of Ti in the (βB) phase is very small, in the assessment (βB) was treated as pure boron and the Gibbs energy was taken from Dinsdale [46].

4. Thermodynamic optimization

The optimization of thermodynamic parameters has been carried out with the help of the PARROT module of Thermo-Calc software developed by Sundman et al. [49]. The working strategy is the minimization of the square sum of the difference between experimental data and computed values. According to Yong Du et al. [50], the key to the successful optimization by using the PARROT program strongly depends on: (i) the models selected for the phases, (ii) how many and which of the model parameters can be assessed with the experimental data available, and (iii) the start values for most of the model parameters.

The optimization started with the stoichiometric TiB and TiB_2. Since there are data available for C_p(TiB) [35], C_p(TiB_2) [35–41], $S_{298\,K}$(TiB) [42], $S_{298\,K}$(TiB_2) [1,35], $\Delta^\circ H_f^{TiB}$(298 K) [42], and $\Delta^\circ H_f^{TiB_2}$(298 K) [1,2,26,42–45],

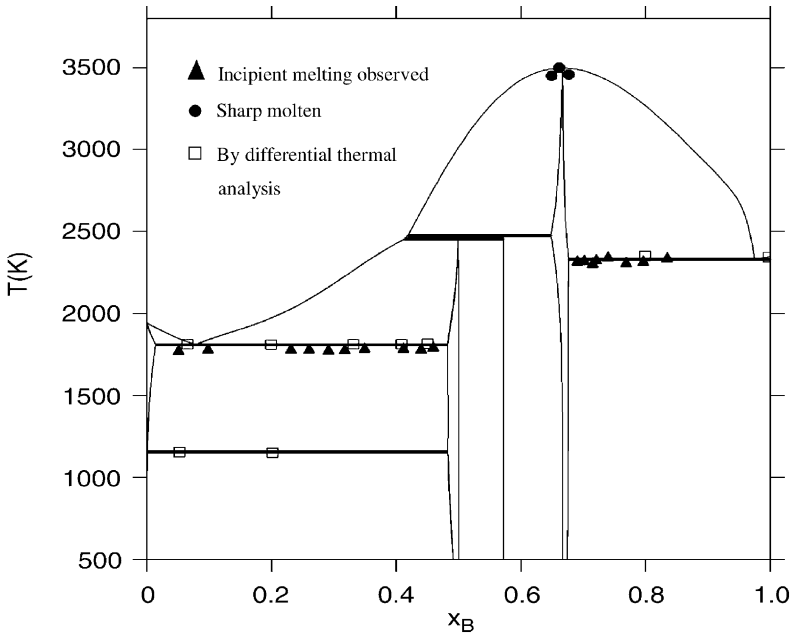

Fig. 3. The Ti–B phase diagram compared with experimental data [9].

Table 4
The optimized thermodynamic parameters of the Ti–B system[a]

Phases	Models	Parameters
Liquid	(B, Ti)$_1$	${}^0L^{\mathrm{L}}_{\mathrm{B,Ti}} = -302969.81 + 35.437T$ ${}^1L^{\mathrm{L}}_{\mathrm{B,Ti}} = -227621.89 + 69.09T$ ${}^2L^{\mathrm{L}}_{\mathrm{B,Ti}} = 57879.33$ ${}^3L^{\mathrm{L}}_{\mathrm{B,Ti}} = 53127.73$
(βTi)	(Ti%)$_1$(B, Va%)$_3$	${}^\circ G^{\beta}_{\mathrm{Ti:B}} - {}^\circ G^{\mathrm{hcp}}_{\mathrm{Ti}} - 3{}^\circ G^{\beta}_{\mathrm{B}} = -174000.24 + 34T$ ${}^0L^{\beta}_{\mathrm{Ti:B,Va}} = -160162.96{+}30T$
(αTi)	(Ti%)$_1$(B, Va%)$_{0.5}$	${}^\circ G^{\alpha}_{\mathrm{Ti:B}} - {}^\circ G^{\mathrm{hcp}}_{\mathrm{Ti}} - 0.5{}^\circ G^{\beta}_{\mathrm{B}} = -50,000$ ${}^0L^{\alpha}_{\mathrm{Ti:B,Va}} = -5071.6$
TiB	(Ti%)$_1$ (B%, Ti)$_1$	${}^\circ G^{\mathrm{TiB}}_{\mathrm{Ti:B}} = -202900 + 338.5T - 53.23T\ln(T) - 0.000286135T^2 + 1090840T^{-1}$ ${}^\circ G^{\mathrm{TiB}}_{\mathrm{Ti:Ti}} - 2{}^\circ G^{\mathrm{hcp}}_{\mathrm{Ti}} = 40,000$ ${}^0L^{\mathrm{TiB}}_{\mathrm{Ti:B,Ti}} = -35924.76 + 24T$
TiB_2	(B, Ti%)$_1$ (B%, Ti)$_2$	${}^\circ G^{\mathrm{TiB_2}}_{\mathrm{B:B}} - 3{}^\circ G^{\beta}_{\mathrm{B}} = 100,000$ ${}^\circ G^{\mathrm{TiB_2}}_{\mathrm{B:Ti}} - {}^\circ G^{\beta}_{\mathrm{B}} - 2{}^\circ G^{\mathrm{hcp}}_{\mathrm{Ti}} = 0$ ${}^\circ G^{\mathrm{TiB_2}}_{\mathrm{Ti:B}} = -338007.94 + 370.83T - 56.4T\ln(T) - 0.01295T^2 + 875000T^{-1} + 0.000000417T^3$ ${}^\circ G^{\mathrm{TiB_2}}_{\mathrm{Ti:Ti}} - 3{}^\circ G^{\mathrm{hcp}}_{\mathrm{Ti}} = 18,000$ ${}^0L^{\mathrm{TiB_2}}_{\mathrm{B:B,Ti}} = -10273.555 + 10T$ ${}^0L^{\mathrm{TiB_2}}_{\mathrm{Ti:B,Ti}} = -10273.555 + 10T$ ${}^0L^{\mathrm{TiB_2}}_{\mathrm{B,Ti:B}} = -103672.21 + 30T$ ${}^0L^{\mathrm{TiB_2}}_{\mathrm{B,Ti:Ti}} = -103672.21 + 30T$
Ti_3B_4	Ti_3B_4	${}^\circ G^{\mathrm{Ti_3B_4}}_{\mathrm{Ti:B}} - 4{}^\circ G^{\beta}_{\mathrm{B}} - 3{}^\circ G^{\mathrm{hcp}}_{\mathrm{Ti}} = -700300 + 15.99T + 5.44T\ln(T)$

[a] In J/(mole of formula units); temperature (T) in Kelvin. The Gibbs energies for the stable forms of boron and titanium (${}^\circ G^{\beta}_{\mathrm{B}}$, ${}^\circ G^{\mathrm{hcp}}_{\mathrm{Ti}}$) are from the SGTE compiled by Dinstale [46]. Percentage means the major component in the related sublattice.

the parameters from a to f in the expressions of ${}^\circ G^{\mathrm{TiB}}_{\mathrm{Ti:B}}$ and ${}^\circ G^{\mathrm{TiB_2}}_{\mathrm{Ti:B_2}}$ can be derived according to the rules of thermodynamics.

Corresponding to the expression of the Gibbs energy of stoichiometric compound in Eq. (1), the heat capacity can be described with the following expression:

$$C_p = -c - 2dT - 2eT^{-2} - 6fT^2 \quad (11)$$

Chase [35] estimated the heat capacities for stoichiometric TiB from 298.15 to 4000 K. Those data were used in the present assessment to fit the following polynome:

$$C_p(\mathrm{TiB}) = 53.23 + (57.28 \times 10^{-5})T - (21.82 \times 10^5)T^{-2} \quad (\mathrm{J\,mol^{-1}\,K^{-1}})$$

where mol refers to one mole of TiB. The predicted heat capacities for stoichiometric TiB are shown in Fig. 2, where the solid line represents the calculated value of this assessment and the circles represent the predicted data from Chase [35].

For stoichiometric TiB_2, Murray et al. [5] fitted the experimental data summarized by Chase with the following polynome:

$$C_p(\mathrm{TiB_2}) = 55.64 + (25.9 \times 10^{-3})T - (17.5 \times 10^5)T^{-2} - (2.5 \times 10^{-6})T^2$$

Table 5
Invariant reactions in the assessed phase diagram

Reaction	Compositions, x_{B}			T (K)	Type
Liquid ↔ TiB_2		0.667		3498	Congruent
Liquid + TiB_2 ↔ Ti_3B_4	0.419	0.65	0.571	2477	Peritectic
Liquid + Ti_3B_4 ↔ TiB	0.413	0.571	0.50	2453	Peritectic
Liquid ↔ TiB_2 + (βB)	0.975	0.676	1.00	2330	Eutectic
Liquid ↔ (βTi) + TiB	0.075	0.008	0.483	1805	Eutectic
(βTi) + TiB ↔ (αTi)	4.90×10^{-4}	0.483	9.29×10^{-4}	1156	Peritectoid
Liquid ↔ (βTi)		0		1943	Melting point
(βTi) ↔ (αTi)		0		1156	Allotropic transformation
Liquid ↔ (βB)		100		2365	Melting point

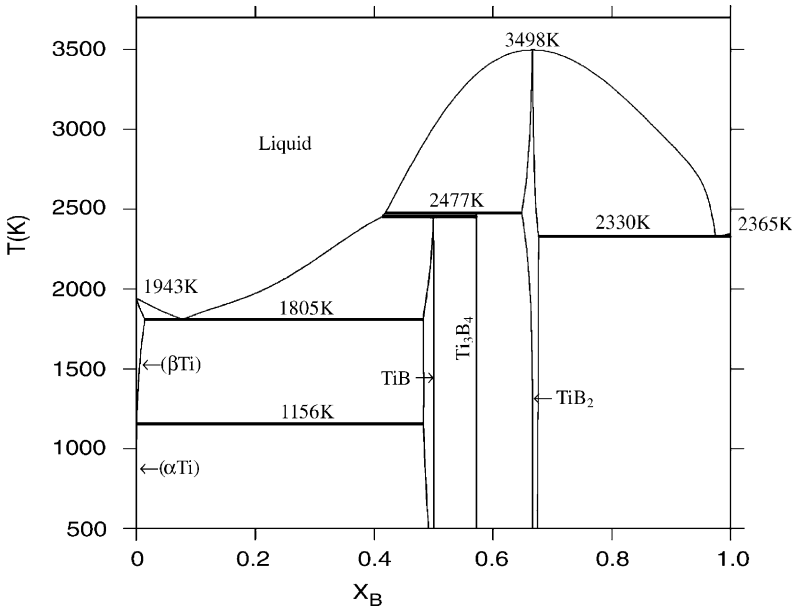

Fig. 4. The Ti–B phase diagram calculated with the present description.

So, the values of *c*, *d*, *e*, *f* were derived directly from the expression of heat capacity and they were used as initial values in the assessment for stoichiometric compound TiB and TiB_2.

5. Results and discussion

The thermodynamic description and the diagram information of the Ti–B system obtained in the present assessment are listed in Tables 4 and 5, respectively.

Fig. 3 shows the comparison of the calculated phase diagram with the experimental data. Satisfactory agreement is obtained. The temperature differences of all the invariant reactions between the thermodynamic prediction and the practical measurement are within experimental uncertainty.

Fig. 4 is the calculated phase diagram with all the critical temperatures labeled.

Figs. 5 and 6 present, respectively, the comparison between the computed results and the experimental data for the entropy $S_{298\,K}$, and the heat of formation $\Delta^{\circ}H_f(298\,K)$ of all the compounds in the Ti–B binary system.

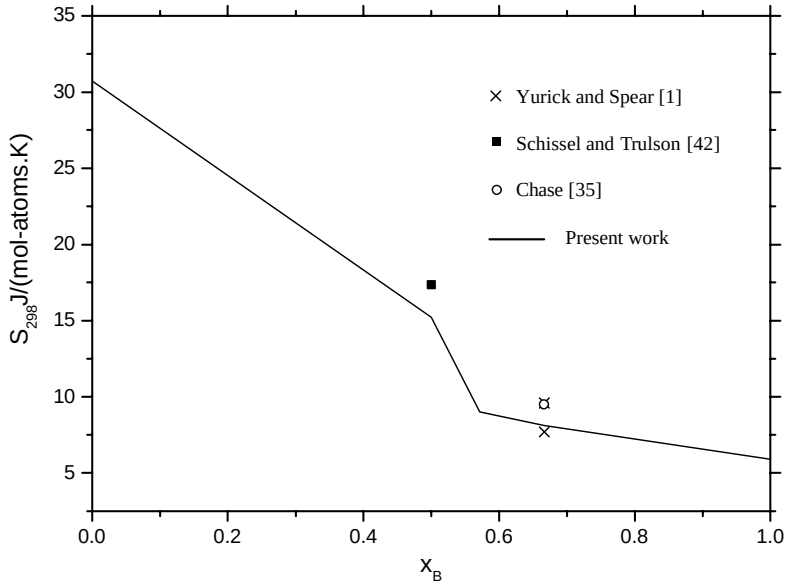

Fig. 5. Calculated entropy at 298 K compared with the experimental data.

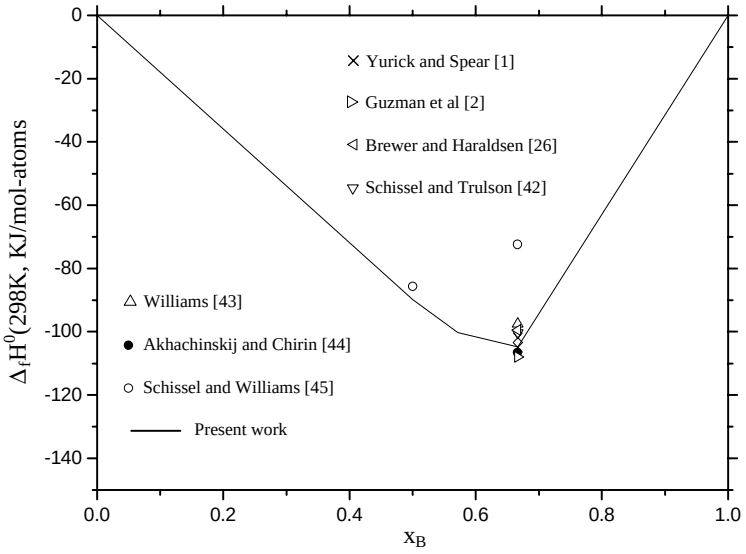

Fig. 6. Calculated enthalpy of formation at 298 K compared with the experimental data.

6. Conclusions

All of the phase equilibrium and thermodynamic data from literature for the Ti–B system have been critically evaluated.

In the meanwhile, the estimated data from Chase [35] are used to fit the polynomial expression for the heat capacity of stochiometric TiB, which is used in turn to predict the parameters in the Gibbs energy expression of TiB.

The evaluated data as well as the result of the present curve fitting are taken into account in this assessment. A consistent thermodynamic data set is obtained after the rigorous optimization by means of CALPHAD technology.

The calculated results are compared with the experimental data. The differences are within experimental uncertainty. Satisfactory agreement is achieved.

Acknowledgements

The authors would like to express their appreciation to the Royal Institute of Technology, Sweden for supplying the Thermo-Calc software. This work was supported by the National Natural Science Foundation of China (no. 50071008).

References

[1] T.J. Yurick, K.E Spear, Thermodynamics of Nuclear Materials 1979, vol. I, IAEA-SM-236/53, 1980, pp. 73–90
[2] L. Guzman, M. Elena, A. Miotello, P.M. Ossi, Vacuum 46 (1995) 951–954.
[3] H. Deng, J. Chen, R.B. Inturi, et al., Surf. Coat. Technol. 76/77 (1995) 609–614.
[4] M. Cirakoglu, S. Bhaduri, S.B. Bhaduri, J. Alloys Compd. 347 (2002) 259–265.
[5] J.L. Murray, P.K. Liao, K.E. Spear, Phase Diagrams of Binary Titanium Alloys, 1987, pp. 33–38
[6] C. Bätzner, 'System B-Ti', COST507, in: I. Ansara, A.T. Dinsdale, M.H. Rand (Eds.), Thermochemical Database For Light Metal Alloys, European Commission, Luxembourg, 1998.
[7] B.F. Decker, J.S. Kasper, Acta Crystallogr. 7 (1954) 77–80.
[8] R.G. Fenish, Phase Relationships in the Titanium–Boron System, NRM-138, 1964, pp. 1–37
[9] E. Rudy, S. Windisch, Ternary Phase Equilibria in Transition Metal–Boron–Carbon–Silicon Systems. Part I. Related Binary System, Ti–B System, vol. VII, Technical Report No. AFML-TR-65-2, Part I, vol. VII, 1966.
[10] J. Thebault, R. Pailler, G. Bontemps-Moley, M. Bourdeau, R. Naslain, J. Less-Common Met. 47 (1976) 221–233.
[11] J.J. Gebhardt, R.F. Cree, J. Am. Ceram. Soc. 48 (5) (1965) 262–267.
[12] H.R. Ogden, R.I. Jaffee, Trans. AIME 191 (1951) 335–336.
[13] A.E. Palty, H. Margolin, J.P. Nielsen, Trans. ASM 46 (1954) 312–328.
[14] H. Okamoto, T.B. Massalski, J. Phase Equilib. 22 (2) (1991) 148–168.
[15] P. Schwarzkopf, F.W. Glaser, Z. Metallkd. 44 (1953) 353–358 (in German).
[16] A. Wittmann, H. Nowotny, H. Boller, Monatsh. Chem. 91 (1960) 608–615.
[17] R.G. Fenish, Trans. AIME 236 (1966) 804.
[18] V.A. Neronov, M.A. Korchagin, V.V. Aleksandrov, S.N. Gusenko, J. Less-Common Met. 82 (1981) 125–129.
[19] K.E. Spear, P. McDowell, F. McMahon, J. Am. Ceram. Soc. 69 (1) (1986) C4–C5.
[20] I.I. Lskoldsky, L.R. Bogorodskaya, Zh. Prikl. Khim., 30 (1957) 177–185 (in Russian); TR: J. Appl. Chem. USSR 30 (1957) 181–188.
[21] R. Kieffer, F. Benesovsky, E.R. Honak, Z. Anorg. Chem. 268 (1952) 191–200.
[22] F.W. Glaser, Trans. AIME 194 (1952) 391–396.
[23] B. Post, F.W. Glaser, D. Moskowitz, Acta Metall. 2 (1954) 20–25.
[24] H. Holleck, J. Vac. Sci. Technol. A 4 (6) (1986) 2661–2669.
[25] B. Post, F.W. Glaser, J. Chem. Phys. 20 (1952) 1050–1051.
[26] L. Brewer, H. Haraldsen, J. Electrochem. Soc. 102 (1955) 399–406.
[27] H.M. Greenhouse, O.E. Accountius, H.H. Sisler, J. Am. Ceram. Soc. 73 (1951) 5086–5087.
[28] P. Villars, L.D. Calvert, Pearson's Handbook of Crystallographic Data for Intermetallic Phases, vol. 2, ASM, Materials Park, OH, 1991.
[29] L. Brewer, D.L. Sawyer, D.H. Templeton, C.H. Dauben, J. Am. Ceram. Soc. 34 (1951) 173–179.

[30] L. Kaufman, E.V. Clougherty, Investigation of boride compounds for high temperature applications, in: F. Benesovsky (Ed.), Plansee Proceedings 1964 on Metals for the Space Age, Plansee Metallwerk, Reutte, Austria, 1965, pp. 722–758.
[31] B. Callmer, Acta Crystallogr. B 33 (1977) 1951–1954.
[32] P. Ehrlich, Z. Anorg. Chem. 259 (1949) 1–41 (in German).
[33] L.H. Andersson, R. Kiessling, Acta Chem. Scand. 24 (1950) 160–164.
[34] J.T. Norton, H. Blumenthal, S.J. Sindeband, Metall. Trans. 185 (1949) 749–751.
[35] M.W. Chase, NIST-JANAF Thermochemical Tables, fourth ed., American Institute of Physics for the National Institute of Standards and Technology, 1998.
[36] B. Wallker, C. Ewing, R. Miller, J. Phys. Chem. 61 (1957) 1682–1683.
[37] A.N. Krestovnikov, M.S. Vendrikh, Izv. V.U.Z. Tsvetn. Metall. 2 (1959) 54–57 (in Russian).
[38] R. Mezaki, E. Tilleux, D.W. Barnes, J.L. Margrave, Thermodynamics of Nuclear Materials, IAEA, Vienna, 1962, pp. 775–788.
[39] R.A. McDonald, F.D. Oetting, H. Prophet, Report No. N64-18824, Dow Chemical Co., Midland, MI, 1963.
[40] D.S. Neel, C.D. Pears, S. Oglesby, Tech. Doc. Report No. ASD-TDR-62-765, Southern Research Institute, Birmingham, AL, 1963.
[41] V.A. Kirilin, A.E. Sheindlin, V.Y. Chekhovskoi, V.I. Tyukaev, Enthalpy and Heat Capacity of Titanium Diboride at 273.15–2600 K, Teplofiz. Vys. Temp. 2 (1964) 710–715 (in Russian)
[42] P.O. Schissel, O.C. Trulson, J. Phys. Chem. 66 (1962) 1492–1496.
[43] W. Williams, J. Phys. Chem. 65 (1961) 2213–2216.
[44] V.V. Akhachinskij, N.A. Chirin, Thermodynamic of Nuclear Materials 1974, vol. II, IAEC, Vienna, 1975, pp. 467–476
[45] P.O. Schissel, W.S. Williams, Bull. Am. Phys. Soc. Ser. II 4 (3) (1959)
[46] A.T. Dinsdale, Calphad 15 (4) (1991) 317.
[47] S. Jonsson, Z. Metallkd. 87 (9) (1996) 691–702.
[48] M. Hillert, L.I. Staffansson, Acta. Chem. Scand. 24 (10) (1970) 3618–3626.
[49] B. Sundman, S. Jansson, J.O. Anderson, Calphad 9 (1985) 153–190.
[50] D. Yong, S.F. Rainer, O. Hiroshi, Z. Metallkd. 88 (7) (1997) 545–556.